

State-aware Re-identification Feature for Multi-target Multi-camera Tracking

Peng Li^{*1,3}, Jiabin Zhang^{*2}, Zheng Zhu^{*2}, Yanwei Li², Lu Jiang³, Guan Huang³

¹Beijing University of Posts and Telecommunications, Beijing, China

²Institute of Automation, Chinese Academy of Sciences, Beijing, China

³Horizon Robotics, Beijing, China

qqilipeng@bupt.edu.cn zhengzhu@ieee.org

{zhangjiabin2016, liyanwei2017}@ia.ac.cn

{lu.jiang, guan.huang}@horizon.ai

Abstract

Multi-target Multi-camera Tracking (MTMCT) aims to extract the trajectories from videos captured by a set of cameras. Recently, the tracking performance of MTMCT is significantly enhanced with the employment of re-identification (Re-ID) model. However, the appearance feature usually becomes unreliable due to the occlusion and orientation variance of the targets. Directly applying Re-ID model in MTMCT will encounter the problem of identity switches (IDS) and tracklet fragment caused by occlusion. To solve these problems, we propose a novel tracking framework in this paper. In this framework, the occlusion status and orientation information are utilized in Re-ID model with human pose information considered. In addition, the tracklet association using the proposed fused tracking feature is adopted to handle the fragment problem. The proposed tracker achieves 81.3% IDF1 on the multiple-camera hard sequence, which outperforms all other reference methods by a large margin.

1. Introduction

Multi-target Multi-camera Tracking (MTMCT) is a significant problem in computer vision and is particularly useful for public security and video understanding [64, 65]. MTMCT aims to track multiple targets across multiple cameras, which is different from the multi-object tracking (MOT) in single camera [49]. Camera network has a broader view than a single camera and has a broader foreground of applications. However, in addition to facing the same challenges of occlusion, pose variance and background clutter with MOT, MTMCT also faces some specific challenges like the blind area among cameras, change of viewpoint and illumination variance.

Feature representation, occlusion handling, and inference are critical components for both MOT and MTMCT. In this paper, we concentrate on the first two components. Appearance feature is significant to maintain the identity of the tracked target, and many works [9, 63, 13] have exploited the reliable appearance model. In specific, color histogram [33, 20] and HOG [27, 7] are well studied and utilized in previous works. However, color histogram and HOG are not robust to the occlusion, and they can not handle the appearance variance well. Recently, re-identification (Re-ID) model is widely adopted as a discriminative appearance descriptor. Besides, person Re-ID is closely related to MTMCT, so the high-quality Re-ID feature always leads to a high tracking performance, which has been proved in [38]. However, Re-ID training data is usually labeled manually, and highly occluded samples are always discarded from the training data. Therefore, using the Re-ID feature directly with the low-quality detector in a crowded scenario always leads to inferior performance.

Occlusion is perhaps the most critical challenge in MOT. It is a primary cause for ID switches or fragmentation of trajectories [31]. Directly extracting the feature from the detection region where the target is highly occluded is unreasonable. Therefore, occlusion awareness is crucial for feature extraction. If occlusion status is obtained, only the stable feature can be retained and the occluded feature can be discarded. Besides, orientation has a significant influence on target appearance, which is neglected by most Re-ID models. In [23], the orientation cue is fully exploited. Specifically, the orientation aware loss is proposed to handle the inconsistent problem by orientation variance. In this work, an orientation-aware feature is used to deal with the inconsistent problem.

In the training process of Re-ID task, one identity contains a limited number of instances, but the length of a trajectory in the tracking scene is not limited. Methods like [13] and [53] adopt latest Re-ID feature to represent the ap-

^{*}The first three authors contributed equally to this work.

pearance feature of trajectory. Besides, [59] utilizes the averaged Re-ID feature as a stable representation, which is a common way to use Re-ID feature. However, appearance varies primarily due to the change of background, pose variance, orientation and viewpoints change. Most existing Re-ID models can not handle these problems. Therefore, post-processing on the Re-ID features is necessary for tracking.

Online trackers [2, 58, 9] build the trajectories with the frame by frame association and they usually only consider the relationship between the trajectories and detections. However, the detection result of the occluded target is always inaccurate, and online trackers may produce many fragmented trajectories in this situation. Unlike online trackers, offline trackers like [48] generate the short tracklets at first and link tracklets to get the final trajectories. In addition, offline trackers usually achieve better performance on account of that they can obtain the entire sequence beforehand, and tracklets contain more information than detections when associating. In this work, the tracklet association is adopted to handle the tracklet fragment.

We focus on handling the above issues. The state-aware Re-ID feature is proposed which focuses on appearance representation with extra human pose information. Specifically, human pose information is utilized to estimate the target state which includes the occlusion status and orientation for making better use of the Re-ID feature. Fused tracking feature is designed as the appearance representation of the tracklet for the stable and accurate association in tracking. A distance matrix with the fused tracking feature is proposed for data association. To handle the fragment of trajectory, the tracklet association is proposed, which includes tracklet rectifying and tracklet clustering. At last, the effectiveness of our framework is verified in the experiment.

The contributions of the paper are listed as follows:

First, human pose information is adopted to infer the target state including the occlusion status and orientation. The novel fused tracking feature is proposed to make the tracking procedure more robust in the crowded scene.

Second, a redesigned distance matrix on data association is proposed to effectively address the occlusion problem. Besides, a novel tracklet association method is designed to deal with the tracklet fragment problem.

Third, our MTMCT tracker with the state-aware Re-ID feature achieves a new state-of-the-art result on Duke MTMCT benchmark [37]. Specifically, the submitted result achieves 81.3 % IDF1 on the multiple-camera hard sequence.

2. Related Works

In this section, we introduce previous works on single camera tracking, multiple camera tracking and appearance feature.

2.1. Single camera tracking

With the development of object detection, data association is widely adopted in a tracking-by-detection framework. Many methods attempt to adopt global optimization as offline methods like [51, 40, 39, 44, 45, 11, 43, 1, 48]. On the other hand, some methods try to solve data association in an online manner like [41, 58, 15, 55, 14, 42, 53, 9]. Offline methods usually generate short but accurate tracklets then construct a graph on them and search optimum solution on the graph to get final trajectories. In [11], Dehghan *et al.* consider all pairwise relationship between targets and models the data association as a Generalized Maximum Multi Clique problem (GMMCP). In [43], Tang *et al.* formulate the data association as a minimum cost subgraph multicut problem. The graph can link the detections across space and time to handle the long term occlusion.

On the other hand, online methods usually match the maintained tracklets with the detections frame by frame. In [55], Xiang *et al.* use the decision making in Markov decision processes to formulate the online MOT, and reinforcement learning is adopted to learn the similarity function. In [58], Yu *et al.* propose a simple tracking pipeline with high-quality detection and deep learning based appearance feature, which leads to an excellent tracking result. The tracking-by-detection framework heavily depends on the detection quality. With the development of single object tracking (SOT) [24, 66, 68, 28, 67, 4], some MOT methods [9, 63] with SOT are proposed to handle the problems caused by the inaccurate detections. In [9], Chu *et al.* introduce the SOT in MOT framework, and spatial-temporal attention mechanism (STAM) is adopted to handle the drift problems caused by SOT. In [63], Zhu *et al.* propose an extended Efficient Convolution Operators (ECO) [10] with cost-sensitive tracking loss and introduce Dual Matching Attention Networks (DMAN) with both spatial and temporal attention mechanisms for data association.

2.2. Multiple cameras tracking

Multi-target Multi-camera Tracking is a challenging task due to the illumination variance, change of viewpoints and the blind area among cameras. Methods like [26, 34, 54, 16, 6, 32] aim to model the relationship among cameras including illumination changes, travel time and entry/exit rates across pairs of cameras. Illumination always varies largely on different viewpoints, so the brightness transfer function (BTF) from a given camera to another camera is estimated to model the illumination changes. [22] finds that all BTFs lie in a low dimensional subspace, and demonstrates that subspace can be used to compute appearance similarity. [36] employs a Cumulative Brightness Transfer Function (CBTF) for mapping color among cameras located at different physical sites. However, the above methods only address the appearance information but ignore the

spatial relationship among cameras. To solve this problem, [21] uses kernel density estimation to infer the inter-camera relationships in the form of the multivariate probability density of space-time variables, then integrates spatial cue and appearance cue with the maximum likelihood estimation framework.

In addition, numerous graph-based models [19, 5, 46, 30, 52, 56, 47] are proposed to deal with MTMCT. [19] constructs a mini-cost flow graph to complete data association among cameras in 3D world space. In [5], the data association is formulated as a constrained flow optimization of a convex problem, and the problem is solved by the k-shortest paths algorithm. In [56], Yoon *et al.* exploit the multiple hypothesis tracking (MHT) algorithm and apply it on MTMCT with some modifications. Branches in track-hypothesis trees represent the trajectory across multiple cameras. Maximum Weight Independent Set (MWIS) in [35] is adopted for computing the best hypothesis set. With the development of Re-ID, a number of methods [56, 30, 30, 59, 38] adopt Re-ID technology to represent the appearance of the target. In [38], Ristani *et al.* learn a good feature for both MTMCT and Re-ID with a convolutional neural network. In [59], Zhang *et al.* obtain a good result with simple hierarchical clustering and well-trained Re-ID feature.

2.3. Appearance feature

In the context of appearance feature, many works [38, 8, 13, 63, 3, 57] recently adopt deep learning to represent appearance of the target. In [13], Feng *et al.* design a quality-aware mechanism to select the K images from the historical samples of the target, and ResNet-18 [17] is adopted to measure the quality of the detection. Then the Re-ID features of the selected detections are input into a classifier to get the similarity score between tracklets and detections. In [63], spatial and temporal attention mechanism are adopted in feature extraction, which make the network focus on the matching patterns of the input image pair. In [9], Chu *et al.* use spatial and temporal attention mechanism on feature extraction to handle the drift problem caused by single object tracker. In [57], Yoon *et al.* apply historical appearance matching to overcome the temporal error. The above methods attempt to solve the problems caused by occlusion and background clutter, and they maintain a stable appearance feature in a complex environment. In this paper, we employ the human pose information to estimate the target state including the occlusion status and orientation. In this way, we can make better use of Re-ID feature.

3. Proposed Method

The overall design for MTMCT is introduced in this section. The proposed tracking framework consists of two parts: single camera tracking (SCT) and multiple camera

tracking (MCT). In our work, the SCT tracker is utilized to generate trajectories in a single camera. Then a similar strategy as [59] is adopted to cluster in-camera trajectories, and the final trajectories are obtained across multiple cameras.

The estimation of occlusion status and orientation are introduced in Sec 3.1, and the fused tracking feature is described in Sec 3.2. The overall SCT framework is presented in Sec 3.3. Finally, MCT tracker is presented in Sec 3.4.

3.1. State estimation

Occlusion status and orientation are estimated with the human pose information. Inference of the occlusion status and orientation is detailed as follows.

Occlusion status estimation Human keypoints can be utilized to infer the occlusion status by the number of keypoints (N_{valid}) which are not occluded. And N_{valid} is computed as:

$$N_{valid} = \sum_{i=1}^{N_k} \mathbb{1}\{c_i > \gamma_{valid}\} \quad (1)$$

where γ_{valid} is the threshold for the confidence of keypoint k_i to judge if k_i is visible, $\mathbb{1}$ equals 1 if the condition is true otherwise 0.

Re-ID feature is regarded as *valid* when N_{valid} is greater than the number threshold (θ_{valid}), which means that most of keypoints are visible and the target is not occluded, otherwise Re-ID feature is regarded as *invalid*.

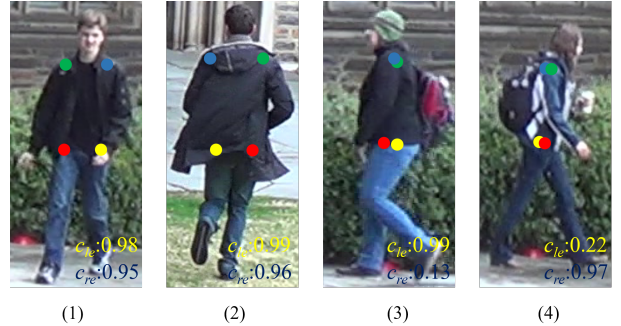


Figure 1. 4 orientations: (1) front, (2) back, (3) left and (4) right. The blue, green, red and yellow points represent the left shoulder, right shoulder, left hip and right hip keypoints respectively.

Orientation estimation Orientation is an important cause for the appearance inconsistency of the same target. As illustrated in Fig. 1, orientation can be easily estimated with body keypoint set $K_{body} = \{k_{ls}, k_{rs}, k_{lh}, k_{rh}\}$ corresponding to left shoulder, right shoulder, left hip, right hip and ear keypoint set $\{k_{le}, k_{re}\}$ corresponding to left ear, right ear. In this work, the orientation is split into four states $O = \{o_{left}, o_{right}, o_{front}, o_{back}\}$, and orientation is

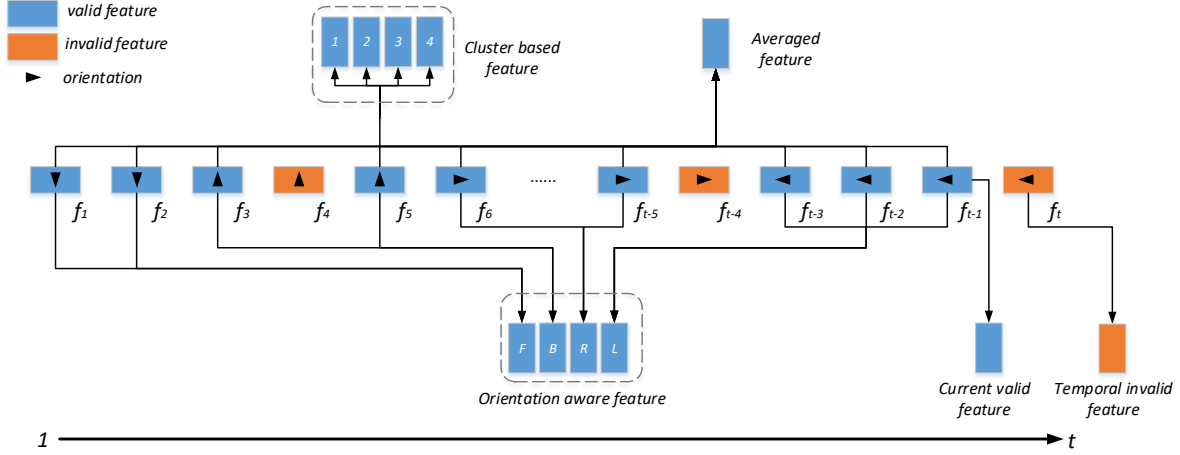


Figure 2. The fused tracking feature consists of current valid feature, temporal invalid feature, orientation-aware feature and averaged feature. Saved historical Re-ID features of the tracklet is shown as $f_1, f_2, \dots, f_{t-1}, f_t$, where f_i is the Re-ID feature from the matched detection d_i in frame i . Four types of orientations including front (F), back (B), left (L) and right (R) are illustrated in f_i . Cluster-based feature is shown with $N_c = 4$. Detailed definition is presented in Sec 3.2.

Table 1. Architecture of the orientation classification network. A simple deep neural network is adopted to divide the input into four orientations. Five fully connected (FC) layers are utilized.

Name	Input size	Output size
FC1	$4 \times 3 + 2$	128
FC2	128	64
FC3	64	128
FC4	128	64
FC5	64	4

inferred with Deep Neural Networks (DNNs) whose architecture is shown in Table 1. Specifically, position and confidence of K_{body} , confidence of ears c_{le}, c_{re} are input into DNN for classification task, so the input dimension is 14.

3.2. Fused tracking feature

Due to the occlusion and variance of orientation, it is hard to model the appearance of the target with the growth of the tracklet. On the other hand, Re-ID model is widely adopted as an advanced appearance descriptor. However, most methods usually use Re-ID feature in a simple way like averaging these features. As shown in Fig. 2, we adopt the well-designed fused tracking feature F_{track} with many different combinations on saved historical Re-ID features of the tracklet, which can represent the appearance of the target more reliably.

The fused tracking feature F_{track} of the tracklet is composed of five types of features as $F_{track} = \{f_{current}, f_{orientation}, f_{cluster}, f_{invalid}, f_{avg}\}$, which is illustrated in the following.

Current valid feature In some scenarios, the target moves fast so that their scale and pose change rapidly. We

use the latest *valid* feature in historical appearances of the target as $f_{current}$ to make the appearance model contain the latest information.

Orientation-aware feature Orientation-aware feature consists of four types of averaged features with different orientations $f_{orientation} = \{f_{left}, f_{right}, f_{front}, f_{back}\}$. Specifically, the feature of $f_{orientation}$ is the mean of all historical *valid* features which have the same orientation.

In data association, one element in $f_{orientation}$ which shares the same orientation with the detection is chosen to compute the appearance distance. Besides, The distance of $f_{orientation}$ between two tracklets is defined as the minimum among the Euclidean distances between the corresponding feature in the same orientation

Cluster-based feature Feature clustering is widely used in non-supervised and semi-supervised Re-ID. In this work, an online cluster algorithm is employed on the cluster-based feature $f_{cluster}$ which has a similar initialization and updating strategy with the Gaussian mixture model. We set N_c as the upper limit of the number of clusters in $f_{cluster}$ and $f_{cluster} = \emptyset$ as initialization. Algorithm 1 details the updating strategy of $f_{cluster}$ when the tracklet matches a detection.

A $N_c \times N_c$ distance matrix $M_{cluster}$ is computed to obtain the distance $d_{cluster}$ between $f_{cluster}$ from two tracklets. Specifically, the value in i -th row and j -th column is the Euclidean distance between the i -th cluster center and j -th cluster center from two tracklets. The minimum value in $M_{cluster}$ is selected as $d_{cluster}$.

Temporal invalid feature When the tracklet matches the detection with *invalid* feature, the above three types of features do not update due to the unreliability of *invalid* fea-

Algorithm 1 Updating $f_{cluster}$

Input: Cluster-based feature is composed of N clusters $f_{cluster} = \{C_1, C_2, \dots, C_N\}$ and detections d with Re-ID feature f_d

Output: updated $f_{cluster}$

```
1: if  $f_d$  is invalid then
2:   return
3: else
4:   if  $N < N_c$  then
5:     new cluster  $C_{N+1}$  is initialized with  $f_d$ ,  $C_{N+1} = \{f_d\}$ 
6:      $C_{N+1}$  is added to  $f_{cluster}$ 
7:   else
8:     Get all cluster centers  $f_{center}$  of  $f_{cluster}$ ,  $f_{center} = \{f_1, f_2, \dots, f_N\}$ 
9:     for  $f_i$  of  $f_{center}$  do
10:       $d_{ci} = \text{dist}(f_i, f_d)$ 
11:     end for
12:      $k = \text{argmin}\{d_{c1}, d_{c2}, \dots, d_{cN}\}$ 
13:     The  $k$ -th cluster  $C_k$  is updated with  $f_d$ 
14:   end if
15: end if
```

ture. However, IDS occurs if the appearance feature is not updated timely. Therefore, temporal invalid feature $f_{invalid}$ is adopted to update the *invalid* feature and make the trajectory more smooth. It is worth noting that that $f_{invalid}$ only keeps the *invalid* feature from the last frame, and will be removed from F_{track} if expired.

Averaged feature Averaged feature f_{avg} is the feature averaged over all *valid* Re-ID feature of the tracklet.

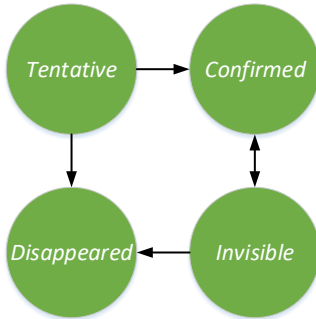


Figure 3. Tracking phase and transformation of the tracklet. *Tentative*, *Confirmed*, *Invisible* and *Disappeared* are four phases of the tracklet lifetime.

3.3. Single camera tracking

3.3.1 Tracking phase

For modeling the lifetime of tracklet in the SCT tracker, we define four phases, *Tentative*, *Confirmed*, *Invisible* and *Disappeared* as shown in Fig. 3. New tracklet is generated

with unmatched detection and initialized to different phase according to the occlusion status. If the detection is highly occluded, the tracking phase will be initialized as *Tentative*. Otherwise, it will be initialized as *Confirmed*. If tracklet in *Confirmed* phase has been missed for μ_m times, it will enter *Invisible* phase. And if tracklet in *Invisible* phase has been missed for μ_d times, it will switch to *Disappeared* phase. Tracklet in *Invisible* phase will go back *Confirmed* phase if the tracklet is matched in data association. Besides, tracklet in *Tentative* phase will turn to *Disappeared* phase if phase misses for one frame, and it will switch to *Confirmed* phase if matches a detection with *valid* feature. In this way, false positive detections can be removed. On the other hand, tracklet in *Disappeared* phase means that the target is disappeared or has already left the scene, so the tracklet is removed from the tracklet set.

3.3.2 Overall SCT framework

In our SCT framework, tracking-by-detection strategy is adopted thanks to the development of object detection. Proposed tracking method follows the nearly online fashion to generate trajectory. Specifically, we maintain a tracklet set from the beginning to the end, and the tracking result is generated after tracklet clustering over every K frames. The SCT framework in this paper can be divided into two parts: tracklets linking and tracklet association, which are shown in Fig. 4 (1) and (2). (1) shows the pipeline which generates and updates tracklets in an online manner. (2) presents the post-processing on tracklets including tracklet rectifying and tracklet clustering. In this way, the tracklet fragment can be handled. Our online SCT framework is shown in detail as follows.

- Step1. At current frame t , detections $D_t = \{d_i^t\}$ are obtained from the high-quality detector, Re-ID feature f_i^t is extracted and keypoints K_i^t of d_i^t are estimated from the corresponding area.
- Step2. Estimate the occlusion status and orientation with the keypoints.
- Step3. Compute the Distance matrix $M_{dis} = \{d_{ij}\}$ between detections and maintained tracklet set.
- Step4. Adopt Hungarian algorithm [25] on M_{dis} to obtain the matching results including matched tracklets $T_{matched}$, unmatched tracklets $T_{unmatched}$ and unmatched detections $D_{unmatched}$.
- Step5. Update $T_{matched}$ with corresponding matched detections.
- Step6. Terminate the tracklets in $T_{unmatched}$ if disappear for a long time. Initialize new tracklets from $D_{unmatched}$ according to the occlusion status.
- Step7. Adopt the tracklet rectifying between tracklets in *Confirmed* phase and tracklets in *Invisible* phase, which are associated if satisfying the designed rule.

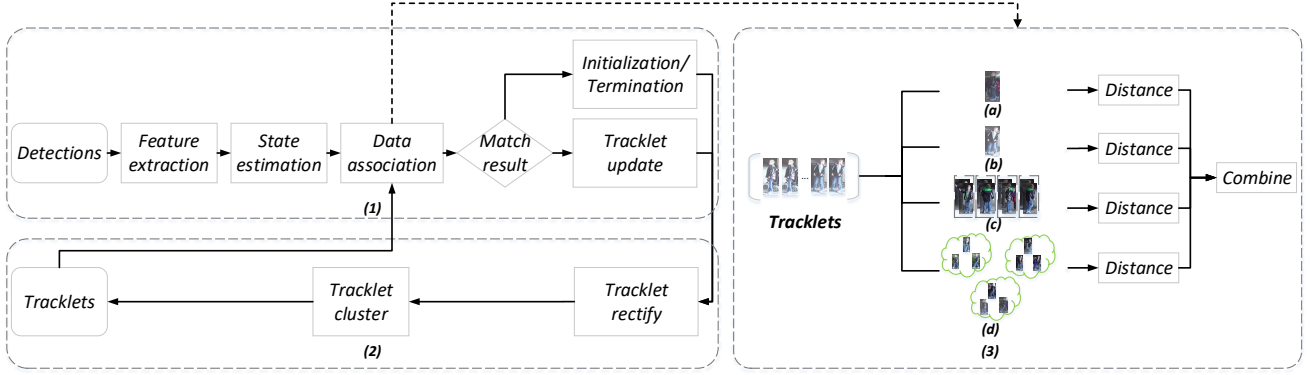


Figure 4. Proposed SCT framework. Overall tracking pipeline is shown in (1) and (2). Specifically, the pipeline of online tracklet generation is presented in (1), and the post-processing on existing tracklets is shown in (2). (3) details the computation of the distance matrix between existing tracklets and detections. (a), (b), (c), (d) are the temporal invalid feature, current valid feature, orientation-aware feature and cluster-based feature respectively. Distance is computed between Re-ID feature from detection and one of the fused tracking feature from tracklet. After that, the final distance between tracklet and detection is combined with the distances of four types of features.

- Step8. Process the tracklet clustering for every K frames in the current tracklet set, and generate the tracking result from the recent K frames after clustering.

3.3.3 Distance matrix in data association

Fig. 4 (3) illustrates the distance between tracklet and detection and Algorithm 2 describes the computation process. At first, elements in M_{dis} are initialized to infinity value. Then we calculate distance between every pair (t_{t-1}^i, d_t^j) . Line 6 uses position information as the spatial constraint to prevent abnormal movement. Line 7 calculates the Euclidean distance between $f_{current}$ and f_{det} . Then the Euclidean distance d_{orien} is calculated by the feature of $f_{orientation}$ which has the same orientation with d_t^j . In line 9, d_{clu} is the minimum Euclidean distance between f_{det} and every cluster center of $f_{cluster}$. In Line 10, $d_{invalid}$ will be computed if $f_{invalid}$ exists of F_{track} and the occlusion status of the detection is *invalid*. Finally the distance m_i^j between t_{t-1}^i and d_t^j is set as the minimum value of d_{curr} , d_{orien} , d_{clu} and $d_{invalid}$.

3.3.4 Tracklet association

Tracklet association is crucial to linking the fragmented tracklets. The proposed tracker can re-track target after occlusion in two ways: tracklet rectifying and tracklet clustering. Before illustrating these two methods, we will introduce the physical constraints to prevent the impossible association and save the computation on constructing the distance matrix.

Physical constraints Three physical constraints are set to prevent the impossible association.

Algorithm 2 Computing distance matrix for data association

Input: tracklets T_{t-1} in frame $t - 1$ and detections D_t in frame t
Output: distance matrix $M_{dis} = \{m_i^j\}$
 initialization: $M_{dis} \leftarrow inf$
 2: **for** each $t_{t-1}^i \in T_{t-1}$ **do**
 for each $d_t^j \in D_t$ **do**
 4: $d_{curr}, d_{orien}, d_{clu}, d_{invalid} \leftarrow inf$
 get Re-ID feature f_{det} , human pose, orientation, occlusion status from d_t^j
 6: check rationality using position information
 $d_{curr} = dist(f_{current}, f_{det})$
 8: $d_{orien} = dist(f_{orientation}, f_{det})$
 $d_{clu} = dist(f_{cluster}, f_{det})$
 10: **if** $f_{invalid}$ exists and f_{det} is *invalid* **then**
 $d_{invalid} = dist(f_{invalid}, f_{det})$
 12: $m_i^j = \min(d_{curr}, d_{orien}, d_{clu}, d_{invalid})$
 else
 14: $m_i^j = \min(d_{curr}, d_{orien}, d_{clu})$
 end if
 end for
 16: **end for**

- Tracklets can not be associated if they appear at the same time.
- Target can not move faster than a threshold. We analyze the position of ground truth and obtain the maximum possible velocity. Given two tracklets, we first sort them by time. The distance between the last detection of the former tracklet and the first detection from the latter one should be less than a maximum distance due to the constraint of velocity.

- Target can not disappear for a long time, so two tracklets can not be associated if the interval between two tracklets is larger than a threshold.

Tracklet rectifying Tracklet rectifying is conducted on the *Invisible* tracklets $T_{invisible}$ and *Confirmed* tracklets $T_{confirmed}$, whose length has reached $L_{rectify}$. Tracklet rectifying aims to re-track the target after occlusion. When the target reappears after occlusion, it may not be matched by the previous tracklet at once, in which case a new tracklet is generated consequently. With the growth of new tracklet, F_{track} becomes more stable, so we can use it to link the fragmented tracklets when the length of the newly generated tracklet reaches $L_{rectify}$. $f_{cluster}$ is adopted to measure the distance between $T_{invisible}$ and $T_{confirmed}$ in the distance matrix $M_{rectify}$. The greedy algorithm is utilized on $M_{rectify}$ to obtain the matched pairs until the minimum distance over $\theta_{rectify}$. At last, the *Invisible* tracklets is associated with corresponding *Confirmed* tracklets according to the matching result.

Tracklet clustering Tracklet clustering aims to associate all the tracklets except the *Disappeared* ones. We follow the same strategy as tracklet rectifying. At first, distance matrix $M_{T-cluster}$ is constructed, then a greedy algorithm is adopted to associate the tracklets with the distance threshold $\theta_{cluster}$. While computing the distance matrix and associating the tracklets, same constraints are adopted. f_{avg} and $f_{orientation}$ are utilized to compute the distance between two tracklets when constructing $M_{T-cluster}$. Specifically, distance between f_{avg} and distance between $f_{orientation}$ are computed as d_{avg} and d_{ori} , and the minor one between d_{avg} and d_{ori} is the final distance between two tracklets.

3.4. Multi-camera tracking

Multi-camera tracking in this work is implemented with a distance matrix M_{mct} and greedy algorithm, which is inspired by [59].

At first, we collect trajectories from all cameras and compute M_{mct} . We follow the same strategy to construct the distance matrix with 3.3.4.

After constructing M_{mct} , the greedy algorithm is adopted to associate trajectories until the minimum distance of the matrix exceeds θ_{mct} . Besides, the same constraints are adopted as [59] when associating trajectories. Different from [59], the distance is updated during associating. Specifically, when a trajectory is associated with others, the corresponding row and column are updated in M_{mct} . In addition, the SCT tracker in this paper is assumed to be good enough, and we only associate the trajectories across different cameras, so the in-camera trajectories stay unchanged.

3.5. Implementation details

Re-ID model We adopt ResNet-34 [18] to extract Re-ID feature. The size of input is 128×256 and 128-d Re-ID feature is extracted from the last fully connected layer. In training process, public Re-ID datasets are used including Market-1501 [60], CUHK03 [29], MSMT17 [50], PRW [61], DukeMTMC-ReID [62] and extra private dataset. The Re-ID model achieves 78.5 Top1 accuracy and 62.4 mAP on DukeMTMC-ReID, whose performance is slightly worse than [54].

Pose estimator In this paper, Alpha pose [12] is adopted to estimate the human pose. Besides, the pose estimator is not fine-tuned on the Duke MTMCT dataset.

Parameter setting For modeling the lifetime of the target, μ_m is set as 10, and μ_d is set as 300. In state estimation, γ_{valid} is set as 0.3, and θ_{valid} is set as 7. In the tracklet association, $\theta_{rectify}$, and $\theta_{cluster}$ are set as 20 and 30. In the multi-camera tracking, θ_{mct} is set as 40.

4. Experiments

In this section, experiments of the proposed state-aware MTMCT framework are conducted. First, the Duke MTMCT dataset and evaluation metric are introduced. Then the effectiveness of our work is proved, and we investigate the contribution of different components. Finally, the result on the test set is submitted, and the proposed tracking framework is compared with other state-of-the-art methods on this benchmark.

4.1. Duke MTMCT dataset

The DukeMTMCT dataset is a large and detailed annotated dataset mainly for MTMCT task, which is recorded in Duke university with 8 cameras. There are 6,791 trajectories for 2,834 different identities overall and 25 minutes for each camera. The dataset is recorded at 60 FPS, and the resolution is 1080p. The dataset is split into three types of parts consisting of *trainval*, *test-easy*, *test-hard*, and *trainval-mini* is the subset of the *trainval*, which contains 59281 frames.

4.2. Evaluation metric

In this work, ID Measure [37] is used as the criterion for both SCT and MTMCT tasks, which can measure the tracker performance globally. The performance evaluation is based on the truth-to-result match. Specifically, it constructs the matching matrix between ground truth and prediction trajectories and uses the Hungarian algorithm to get the final matching result. IDP, IDR and IDF1 are three main metrics for ID Measure. IDP (IDR) is the fraction of prediction (ground truth) detection are correctly identified. IDF1 is the correctly identified detections over the average value of ground truth and prediction.

Table 2. The result of our tracker and several state-of-the-art trackers on test sequence of Duke MTMCT. The value in bold highlight is the best. Tracker MTMC_basel is recently submitted on Duke MTMCT benchmark.

Tracker	<i>test-easy single</i>			<i>test-easy multiple</i>			<i>test-hard single</i>			<i>test-hard multiple</i>		
	IDF1	IDP	IDR	IDF1	IDP	IDR	IDF1	IDP	IDR	IDF1	IDP	IDR
BIPCC[37]	70.1	83.6	60.4	56.2	67.0	48.4	64.5	81.2	53.5	47.3	59.6	39.2
MYTRACKER[56]	80.3	87.3	74.4	65.4	71.1	60.6	63.5	73.9	55.6	50.1	58.3	43.9
TAREIDMTMC[23]	83.8	87.6	80.4	68.8	71.8	66.0	77.9	86.6	70.7	61.2	68.0	55.5
DeepCC[38]	89.2	91.7	86.7	82.0	84.3	79.8	79.0	87.4	72.0	68.5	75.8	62.4
MTMC_ReID[59]	89.8	92.0	87.7	83.2	85.2	81.2	81.2	89.4	74.5	74.0	81.4	67.8
MTMC_basel	91.3	91.8	90.9	87.4	87.8	87.0	83.7	88.8	79.1	75.4	80.0	71.3
Ours	91.8	93.3	90.3	86.8	88.2	85.4	85.8	93.6	79.2	81.3	88.7	75.1

Table 3. Ablation study demonstrates the steady improvements of the state-aware Re-ID feature. IDF1, MOTA and IDS are shown in this table, and the arrows indicate low or high optimal metric values.

Method	IDF1	MOTA	IDS
Baseline	77.1	82.8	6409
Baseline + $f_{cluster}$	82.5	82.6	8170
Baseline + $f_{cluster}$ + $f_{orientation}$	85.1	82.8	6564
Baseline + $f_{cluster}$ + $f_{orientation}$ + $f_{invalid}$	85.2	82.8	5466

4.3. Ablation study

Ablation study is conducted on the SCT task of *trainval-mini* sequences. The orientation-aware feature, cluster-based feature and temporal valid feature are considered. The baseline tracker only uses current valid feature $f_{current}$ for data association and the time interval K to generate tracking result is set as 10 seconds, which means 600 frames in Duke MTMCT dataset. The results of ablation study is shown in Table 3.

Cluster-based feature Comparing the tracker in the second row with baseline, the cluster-based feature is essential, and it can improve the performance on IDF1 by 5.4 %. One can find that current valid feature can not model the target appearance correctly and the cluster-based feature is an effective way to represent the appearance of the target. $f_{cluster}$ becomes more stable with the growth of the tracklet, but is not robust to the occlusion at the beginning, which is the main cause for the increase of IDS.

Orientation-aware feature Comparing the tracker in the third row with the tracker in the second row, the tracker with orientation-aware feature performs better which gains 2.6 % improvement on IDF1. One can find that the orientation feature is complementary with the cluster feature.

Temporal invalid Feature Comparing the tracker in the fourth row with the tracker in the third row, IDF1 is improved by 0.1 %, and IDS is reduced from 6564 to 5466, which means the invalid temporal feature effectively reduces the IDS and makes the trajectory more smooth.

4.4. Compare with other state-of-the-art methods

We compare the proposed tracker with other tracking methods [37, 56, 23, 38, 59] on DukeMTMCT dataset, and results are shown in Table 2.

We utilize the private detection provided by [59], and our tracker achieves a state-of-the-art performance on both *test-easy* and *test-hard* sequences. Besides, we outperform all officially published methods on IDF1 and IDR. We evaluate the proposed tracking method without any training or optimization on the train set, and the same parameters are utilized on *test-easy* and *test-hard* sequences. For the performance comparison, we collect some published methods and recently submitted method (MTMCT_basel) on DukeMTMCT benchmark. For better performance, the offline SCT tracker is adopted, which means the time interval to cluster and output is set as the length of the corresponding sequence. Specifically, tracker first generates short but accurate tracklets and tracklet clustering in Sec. 3.3.4 is adopted to associate these tracklets to obtain the final trajectories.

As shown in Table 2, our tracker achieves a new state-of-the-art performance on DukeMTMCT dataset. Due to the well-designed state-aware Re-ID feature, we outperform all other methods including an unpublished method on the benchmark by a large margin on *test-hard*, which further verifies the robustness of proposed tracker in such crowded scene, as the motion cue becomes unstable when occluded.

5. Conclusion

In this paper, we propose the state-aware Re-ID feature for multiple cameras, multiple targets tracking task. We adopt human pose information to infer the occlusion status and orientation. Besides, the fused tracking feature is designed to make better use of Re-ID feature. Our tracker achieves a new state-of-the-art performance on DukeMTMCT benchmark, which verifies the effectiveness of the proposed method.

References

- [1] Maryam Babaei, Ali Athar, and Gerhard Rigoll. Multiple people tracking using hierarchical deep tracklet re-identification. *arXiv preprint arXiv:1811.04091*, 2018. 2
- [2] Seung-Hwan Bae and Kuk-Jin Yoon. Robust online multi-object tracking based on tracklet confidence and online discriminative appearance learning. In *Conference on computer vision and pattern recognition*, pages 1218–1225, 2014. 2
- [3] Seung-Hwan Bae and Kuk-Jin Yoon. Confidence-based data association and discriminative deep appearance learning for robust online multi-object tracking. *IEEE Transactions on Pattern Analysis and Machine Intelligence*, 40(3):595–610, 2018. 3
- [4] Shuai Bai, Zhiqun He, Ting-Bing Xu, Zheng Zhu, Yuan Dong, and Hongliang Bai. Multi-hierarchical independent correlation filters for visual tracking. *arXiv preprint arXiv:1811.10302*, 2018. 2
- [5] Jerome Berclaz, Francois Fleuret, Engin Turetken, and Pascal Fua. Multiple object tracking using k-shortest paths optimization. *IEEE Transactions on Pattern Analysis and Machine Intelligence*, 33(9):1806–1819, 2011. 3
- [6] Simone Calderara, Rita Cucchiara, and Andrea Prati. Bayesian-competitive consistent labeling for people surveillance. *IEEE Transactions on Pattern Analysis and Machine Intelligence*, 30(2):354–360, 2008. 2
- [7] Wongun Choi and Silvio Savarese. A unified framework for multi-target tracking and collective activity recognition. In *European Conference on Computer Vision*, pages 215–230, 2012. 1
- [8] Peng Chu, Heng Fan, Chiu C Tan, and Haibin Ling. Online multi-object tracking with instance-aware tracker and dynamic model refreshment. In *IEEE Winter Conference on Applications of Computer Vision*, pages 161–170, 2019. 3
- [9] Qi Chu, Wanli Ouyang, Hongsheng Li, Xiaogang Wang, Bin Liu, and Nenghai Yu. Online multi-object tracking using cnn-based single object tracker with spatial-temporal attention mechanism. In *IEEE International Conference on Computer Vision*, pages 4836–4845, 2017. 1, 2, 3
- [10] Martin Danelljan, Goutam Bhat, Fahad Shahbaz Khan, and Michael Felsberg. Eco: Efficient convolution operators for tracking. In *IEEE Conference on Computer Vision and Pattern Recognition*, pages 6638–6646, 2017. 2
- [11] Afshin Dehghan, Shayan Modiri Assari, and Mubarak Shah. Gmmcp tracker: Globally optimal generalized maximum multi clique problem for multiple object tracking. In *IEEE Conference on Computer Vision and Pattern Recognition*, pages 4091–4099, 2015. 2
- [12] Hao-Shu Fang, Shuqin Xie, Yu-Wing Tai, and Cewu Lu. Rmpe: Regional multi-person pose estimation. In *IEEE International Conference on Computer Vision*, pages 2334–2343, 2017. 7
- [13] Weitao Feng, Zhihao Hu, Wei Wu, Junjie Yan, and Wanli Ouyang. Multi-object tracking with multiple cues and switcher-aware classification. *arXiv preprint arXiv:1901.06129*, 2019. 1, 3
- [14] Weihao Gan, Shuo Wang, Xuejing Lei, Ming-Sui Lee, and C-C Jay Kuo. Online cnn-based multiple object tracking with enhanced model updates and identity association. *Signal Processing: Image Communication*, 66:95–102, 2018. 2
- [15] Xu Gao and Tingting Jiang. Osmo: Online specific models for occlusion in multiple object tracking under surveillance scene. In *ACM International Conference on Multimedia*, pages 201–210, 2018. 2
- [16] Andrew Gilbert and Richard Bowden. Tracking objects across cameras by incrementally learning inter-camera colour calibration and patterns of activity. In *European Conference on Computer Vision*, pages 125–136, 2006. 2
- [17] Kaiming He, Xiangyu Zhang, Shaoqing Ren, and Jian Sun. Deep residual learning for image recognition. In *IEEE Conference on Computer Vision and Pattern Recognition*, pages 770–778, 2016. 3
- [18] Kaiming He, Xiangyu Zhang, Shaoqing Ren, and Jian Sun. Deep residual learning for image recognition. In *IEEE Conference on Computer Vision and Pattern Recognition*, pages 770–778, 2016. 7
- [19] Martin Hofmann, Daniel Wolf, and Gerhard Rigoll. Hypergraphs for joint multi-view reconstruction and multi-object tracking. In *IEEE Conference on Computer Vision and Pattern Recognition*, pages 3650–3657, 2013. 3
- [20] Hamid Izadinia, Imran Saleemi, Wenhui Li, and Mubarak Shah. 2 t: multiple people multiple parts tracker. In *European Conference on Computer Vision*, pages 100–114, 2012. 1
- [21] Omar Javed, Khurram Shafique, Zeeshan Rasheed, and Mubarak Shah. Modeling inter-camera space-time and appearance relationships for tracking across non-overlapping views. *Computer Vision and Image Understanding*, 109(2):146–162, 2008. 3
- [22] Omar Javed, Khurram Shafique, and Mubarak Shah. Appearance modeling for tracking in multiple non-overlapping cameras. In *IEEE Conference on Computer Vision and Pattern Recognition*, volume 2, pages 26–33, 2005. 2
- [23] Na Jiang, SiChen Bai, Yue Xu, Chang Xing, Zhong Zhou, and Wei Wu. Online inter-camera trajectory association exploiting person re-identification and camera topology. In *ACM International Conference on Multimedia*, pages 1457–1465, 2018. 1, 8
- [24] Matej Kristan, Aleš Leonardis, Jiří Matas, Michael Felsberg, Roman Pflugfelder, Luka Čehovin Zajc, Tomáš Vojtř, Goutam Bhat, Alan Lukežič, Abdelrahman Eldesokey, et al. The sixth visual object tracking vot2018 challenge results. In *European Conference on Computer Vision*, pages 3–53. Springer, Cham, 2018. 2
- [25] Harold W Kuhn. The hungarian method for the assignment problem. *Naval research logistics quarterly*, 2(1-2):83–97, 1955. 5
- [26] Cheng-Hao Kuo, Chang Huang, and Ram Nevatia. Inter-camera association of multi-target tracks by on-line learned appearance affinity models. In *European Conference on Computer Vision*, pages 383–396, 2010. 2
- [27] Cheng-Hao Kuo, Chang Huang, and Ramakant Nevatia. Multi-target tracking by on-line learned discriminative appearance models. In *IEEE Conference on Computer Vision and Pattern Recognition*, pages 685–692, 2010. 1

- [28] Bo Li, Junjie Yan, Wei Wu, Zheng Zhu, and Xiaolin Hu. High performance visual tracking with siamese region proposal network. In *IEEE Conference on Computer Vision and Pattern Recognition*, pages 8971–8980, 2018. 2
- [29] Wei Li, Rui Zhao, Tong Xiao, and Xiaogang Wang. Deep-reid: Deep filter pairing neural network for person re-identification. In *IEEE Conference on Computer Vision and Pattern Recognition*, pages 152–159, 2014. 7
- [30] Wenqian Liu, Octavia Camps, and Mario Sznai. Multi-camera multi-object tracking. *arXiv preprint arXiv:1709.07065*, 2017. 3
- [31] Wenhan Luo, Junliang Xing, Anton Milan, Xiaoqin Zhang, Wei Liu, Xiaowei Zhao, and Tae-Kyun Kim. Multiple object tracking: A literature review. *arXiv preprint arXiv:1409.7618*, 2014. 1
- [32] Dimitrios Makris, Tim Ellis, and James Black. Bridging the gaps between cameras. In *IEEE Conference on Computer Vision and Pattern Recognition*, 2004. 2
- [33] Dennis Mitzel and Bastian Leibe. Real-time multi-person tracking with detector assisted structure propagation. In *IEEE International Conference on Computer Vision Workshops*, pages 974–981, 2011. 1
- [34] Neeti Narayan, Nishant Sankaran, Devansh Arpit, Karthik Dantu, Srirangaraj Setlur, and Venu Govindaraju. Person re-identification for improved multi-person multi-camera tracking by continuous entity association. In *IEEE Conference on Computer Vision and Pattern Recognition Workshops*, pages 64–70, 2017. 2
- [35] Dimitri J Papageorgiou and Michael R Salpukas. The maximum weight independent set problem for data association in multiple hypothesis tracking. In *Optimization and Cooperative Control Strategies*, pages 235–255. Springer, 2009. 3
- [36] Bryan James Prosser, Shaogang Gong, and Tao Xiang. Multi-camera matching using bi-directional cumulative brightness transfer functions. In *British Machine Vision Conference*, volume 8, page 74, 2008. 2
- [37] Ergys Ristani, Francesco Solera, Roger Zou, Rita Cucchiara, and Carlo Tomasi. Performance measures and a data set for multi-target, multi-camera tracking. In *European Conference on Computer Vision*, pages 17–35, 2016. 2, 7, 8
- [38] Ergys Ristani and Carlo Tomasi. Features for multi-target multi-camera tracking and re-identification. In *IEEE Conference on Computer Vision and Pattern Recognition*, pages 6036–6046, 2018. 1, 3, 8
- [39] Han Shen, Lichao Huang, Chang Huang, and Wei Xu. Tracklet association tracker: An end-to-end learning-based association approach for multi-object tracking. *arXiv preprint arXiv:1808.01562*, 2018. 2
- [40] Hao Sheng, Jiahui Chen, Yang Zhang, Wei Ke, Zhang Xiong, and Jingyi Yu. Iterative multiple hypothesis tracking with tracklet-level association. *IEEE Transactions on Circuits and Systems for Video Technology*, 2018. 2
- [41] Francesco Solera, Simone Calderara, and Rita Cucchiara. Learning to divide and conquer for online multi-target tracking. In *IEEE International Conference on Computer Vision*, pages 4373–4381, 2015. 2
- [42] ShiJie Sun, Naveed Akhtar, HuanSheng Song, Ajmal Mian, and Mubarak Shah. Deep affinity network for multiple object tracking. *arXiv preprint arXiv:1810.11780*, 2018. 2
- [43] Siyu Tang, Bjoern Andres, Miykhaylo Andriluka, and Bernt Schiele. Subgraph decomposition for multi-target tracking. In *IEEE Conference on Computer Vision and Pattern Recognition*, pages 5033–5041, 2015. 2
- [44] Siyu Tang, Bjoern Andres, Mykhaylo Andriluka, and Bernt Schiele. Multi-person tracking by multicut and deep matching. In *European Conference on Computer Vision*, pages 100–111, 2016. 2
- [45] Siyu Tang, Mykhaylo Andriluka, Bjoern Andres, and Bernt Schiele. Multiple people tracking by lifted multicut and person re-identification. In *IEEE Conference on Computer Vision and Pattern Recognition*, pages 3539–3548, 2017. 2
- [46] Yonatan Tariku Tesfaye, Eyasu Zemene, Andrea Prati, Marcello Pelillo, and Mubarak Shah. Multi-target tracking in multiple non-overlapping cameras using constrained dominant sets. *arXiv preprint arXiv:1706.06196*, 2017. 3
- [47] Jiuqing Wan and Liu Li. Distributed optimization for global data association in non-overlapping camera networks. In *International Conference on Distributed Smart Cameras*, pages 1–7, 2013. 3
- [48] Gaoang Wang, Yizhou Wang, Haotian Zhang, Renshu Gu, and Jenq-Neng Hwang. Exploit the connectivity: Multi-object tracking with trackletnet. *arXiv preprint arXiv:1811.07258*, 2018. 2
- [49] Xiaogang Wang. Intelligent multi-camera video surveillance: A review. *Pattern recognition letters*, 34(1):3–19, 2013. 1
- [50] Longhui Wei, Shiliang Zhang, Wen Gao, and Qi Tian. Person transfer gan to bridge domain gap for person re-identification. *arXiv preprint arXiv:1711.08565*, 2017. 7
- [51] Longyin Wen, Dawei Du, Shengkun Li, Xiao Bian, and Siwei Lyu. Learning non-uniform hypergraph for multi-object tracking. *arXiv preprint arXiv:1812.03621*, 2018. 2
- [52] Longyin Wen, Zhen Lei, Ming-Ching Chang, Honggang Qi, and Siwei Lyu. Multi-camera multi-target tracking with space-time-view hyper-graph. *International Journal of Computer Vision*, 122(2):313–333, 2017. 3
- [53] Nicolai Wojke, Alex Bewley, and Dietrich Paulus. Simple online and realtime tracking with a deep association metric. In *IEEE International Conference on Image Processing*, pages 3645–3649, 2017. 1, 2
- [54] Chih-Wei Wu, Meng-Ting Zhong, Yu Tsao, Shao-Wen Yang, Yen-Kuang Chen, and Shao-Yi Chien. Track-clustering error evaluation for track-based multi-camera tracking system employing human re-identification. In *IEEE Conference on Computer Vision and Pattern Recognition Workshops*, pages 1–9, 2017. 2, 7
- [55] Yu Xiang, Alexandre Alahi, and Silvio Savarese. Learning to track: Online multi-object tracking by decision making. In *IEEE International Conference on Computer Vision*, pages 4705–4713, 2015. 2
- [56] Kwangjin Yoon, Young-min Song, and Moongu Jeon. Multiple hypothesis tracking algorithm for multi-target multi-camera tracking with disjoint views. *Image Processing*, 12(7):1175–1184, 2018. 3, 8

- [57] Young-chul Yoon, Abhijeet Boragule, Young-min Song, Kwangjin Yoon, and Moongu Jeon. Online multi-object tracking with historical appearance matching and scene adaptive detection filtering. In *IEEE International Conference on Advanced Video and Signal Based Surveillance*, pages 1–6, 2018. 3
- [58] Fengwei Yu, Wenbo Li, Quanquan Li, Yu Liu, Xiaohua Shi, and Junjie Yan. Poi: Multiple object tracking with high performance detection and appearance feature. In *European Conference on Computer Vision*, pages 36–42, 2016. 2
- [59] Zhimeng Zhang, Jianan Wu, Xuan Zhang, and Chi Zhang. Multi-target, multi-camera tracking by hierarchical clustering: recent progress on dukemtmc project. *arXiv preprint arXiv:1712.09531*, 2017. 2, 3, 7, 8
- [60] Liang Zheng, Liyue Shen, Lu Tian, Shengjin Wang, Jingdong Wang, and Qi Tian. Scalable person re-identification: A benchmark. In *IEEE International Conference on Computer Vision*, pages 1116–1124, 2015. 7
- [61] Liang Zheng, Hengheng Zhang, Shaoyan Sun, Manmohan Chandraker, Yi Yang, Qi Tian, et al. Person re-identification in the wild. In *IEEE Conference on Computer Vision and Pattern Recognition*, 2017. 7
- [62] Zhedong Zheng, Liang Zheng, and Yi Yang. Unlabeled samples generated by gan improve the person re-identification baseline in vitro. In *IEEE International Conference on Computer Vision*, pages 3754–3762, 2017. 7
- [63] Ji Zhu, Hua Yang, Nian Liu, Minyoung Kim, Wenjun Zhang, and Ming-Hsuan Yang. Online multi-object tracking with dual matching attention networks. In *European Conference on Computer Vision*, pages 366–382, 2018. 1, 2, 3
- [64] Jiagang Zhu, Zheng Zhu, and Wei Zou. End-to-end video-level representation learning for action recognition. In *2018 24th International Conference on Pattern Recognition (ICPR)*, pages 645–650. IEEE, 2018. 1
- [65] Jiagang Zhu, Wei Zou, and Zheng Zhu. Two-stream gated fusion convnets for action recognition. In *2018 24th International Conference on Pattern Recognition (ICPR)*, pages 597–602. IEEE, 2018. 1
- [66] Zheng Zhu, Guan Huang, Wei Zou, Dalong Du, and Chang Huang. Uct: Learning unified convolutional networks for real-time visual tracking. In *IEEE International Conference on Computer Vision Workshops*, pages 1973–1982, 2017. 2
- [67] Zheng Zhu, Qiang Wang, Bo Li, Wei Wu, Junjie Yan, and Weiming Hu. Distractor-aware siamese networks for visual object tracking. In *IEEE European Conference on Computer Vision (ECCV)*, pages 101–117, 2018. 2
- [68] Zheng Zhu, Wei Wu, Wei Zou, and Junjie Yan. End-to-end flow correlation tracking with spatial-temporal attention. In *IEEE Conference on Computer Vision and Pattern Recognition*, 2018. 2